Inorganic Chemistry
Article
pubs.acs.org/IC

Heterometallic Alumo- and Gallodisilicates with M(O−Si−O)$_2$M′ and [M(O−Si−O)$_2$]$_2$M′ Cores (M = Al, Ga; M′ = Ti, Zr, Hf)

Raúl Huerta-Lavorie, Diego Solis-Ibarra, Dana Victoria Báez-Rodríguez, Marisol Reyes-Lezama, M. de las Nieves Zavala-Segovia, and Vojtech Jancik*

Centro Conjunto de Investigación en Química Sustentable UAEM-UNAM, Car. Toluca-Atlacomulco km 14.5, Toluca 50200, Estado de México, México

Supporting Information

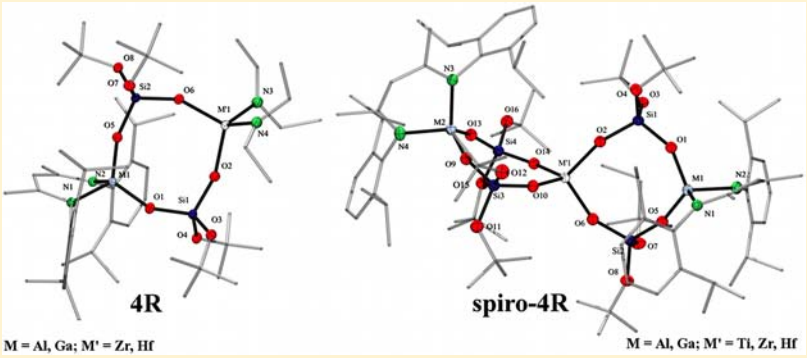

ABSTRACT: The synthesis and stabilization of alumo- and gallodisilicates [HC{C(Me)N(2,6-*i*Pr$_2$C$_6$H$_3$)}$_2$]M[(μ-O)Si(OH)(O*t*Bu)$_2$]$_2$ [M = Al (**1**), Ga (**2**)] containing two silicate subunits have been achieved through reactions between 2 equiv of the silanediol (*t*BuO)$_2$Si(OH)$_2$ and the aluminum hydride [HC{C(Me)N(2,6-*i*Pr$_2$C$_6$H$_3$)}$_2$]AlH$_2$ or the gallium amide [HC{C(Me)N(2,6-*i*Pr$_2$C$_6$H$_3$)}$_2$]Ga(NHEt)$_2$, respectively. Compounds **1** and **2** exhibit M(O−SiO$_2$−OH)$_2$ moiety and represent the first molecular metallosilicate-based analogues of neighboring silanol groups found in silicate surfaces. The substitution of both SiOH groups led to the formation of bimetallic compounds with 4R topologies, which are regularly found in zeolitic materials. Thus, reactions between group 4 metal amides M′(NEt$_2$)$_4$ (M′ = Ti, Zr, Hf) and **1** and **2** resulted in the formation of nine heterometallic silicates (**3**−**11**) containing inorganic M(O−Si−O)$_2$M′ and [M(O−Si−O)$_2$]$_2$M′ cores with 4R and spiro-4R topologies, respectively. The latter have M···M distances of 0.81 nm. NMR studies of the heterometallic derivatives showed a fluxional behavior at room temperature due to a high flexibility of the eight-membered ring.

INTRODUCTION

One of the most important types of natural inorganic compounds containing cyclic subunits are silicates and alumosilicates. These minerals or their synthetic analogues, belonging to the zeolite class, are commercially used in a wide variety of applications such as ion exchange,[1a] catalysis (mainly in the petrochemical industry),[1b,c,g−i] separations (most notably N$_2$ and O$_2$ from air),[1d] and support for nanoparticles among others.[1e] These features are the result of a combination of inorganic rings with different sizes, formed by 6 (3R), 8 (4R), 12 (6R), 16 (8R), 18 (9R), and 24 (12R) atoms, with the 4R and 6R rings being the most common.[1f] The elucidation of the interaction of these rigid frameworks with the precursors is difficult because of the heterogeneous nature of the reactions and the lack of suitable characterization techniques. Therefore, the development of simple systems with similar connectivity is a viable route to overcome these obstacles. In fact, just recently the first heterogeneous 2D-alumosilicate films were proposed as a model for zeolites.[2] Therefore, the use of molecular silicates that resemble the structure of zeolites, but remain as crystalline and soluble compounds, is a promising alternative for the better understanding of these materials. Moreover, molecular models could give valuable insight in the nature of silicate bonding and could eventually serve as building units for hybrid materials, particularly with the recent development of new families of porous materials such as periodic mesoporous organosilicas (PMOs),[3a] silicon based metal−organic frameworks (MOFs),[3b−d] and, more recently, eni-carbon silicates (ECS-s).[3e,f] However, stabilization of simple silicate rings in a molecular form is difficult due to the ease of formation and dissociation of Al−O and Si−O bonds and the high oligomerization tendency of these units.[4] Recently, we have reported on the synthesis of 3R type heterobimetallic alumo- and gallosilicates with M′−O−Si−O−M−O connectivity based on [HC{C(Me)N(2,6-*i*Pr$_2$C$_6$H$_3$)}$_2$]M(OH·thf)(μ-O)Si(OH)(O*t*Bu)$_2$ (M = Al (**a**), Ga (**b**)) precursors with highly reactive M−OH and Si−OH groups in the same molecule (Figure 1).[5]

Received: January 21, 2013
Published: May 29, 2013

dx.doi.org/10.1021/ic400156n | *Inorg. Chem.* 2013, 52, 6934−6943

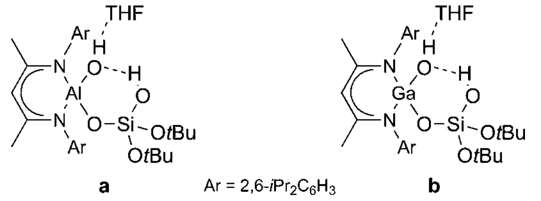

Figure 1. Compounds **a** and **b**.

A similar synthetic strategy may be used for the preparation of simple 4R type heterobimetallic silicate Si−O−M−O−Si−O−M′−O (M, M′ = different metals) rings, which to the best of our knowledge are unknown. Until now, only monometallic compounds with Si_3MO_4 rings[6] and homobimetallic $Si_2M_2O_4$ ring-containing species have been reported.[6a,e,7,8] This is due to a low degree of control over the association reactions and the limited access to the $M(O{-}Si{-}OH)_2$ precursors necessary for the formation of the heterobimetallic 4R systems in a stepwise reactions. To date, only three such compounds have been reported on the basis of aluminum ($[[(2,6\text{-}i\mathrm{Pr}_2C_6H_3)N(SiMe_2\text{-}i\mathrm{Pr})SiO(OH)_2]_2AlC(SiMe_3)_3{\cdot}3THF)$,[9] niobium ($(t\mathrm{Bu}_2Si(O)_2[(t\mathrm{Bu}_2Si(OH)O)_2Nb]_2[C_5Me_4EtNb(Cl)]\mu_2\text{-}Cl)(\mu_2\text{-}O)_2(\mu_3\text{-}O))$,[8] and tin ($[Me_2N(CH_2)_3]_2Sn(OSit\mathrm{Bu}_2OH)_2$),[10] but only the aluminum compound can be prepared in a yield over 40%. Silicon based systems with such vicinal Si−OH groups are restricted to partially hydrolyzed silsesquioxanes,[11] a few acyclic $Si(O{-}Si{-}OH)_2$ siloxanes,[12] and only one example of a silicate $(tBuO)_2Si[(\mu\text{-}O)Si(OtBu)_2(OH)]_2$.[13] None of these have been used for the preparation of bimetallic systems with the desired connectivity. Herein, we report on a facile synthesis of mono- and spirocyclic 4R type heterobimetallic alumo- and gallodisilicates based on the $[HC\{C(Me)N(2,6\text{-}i\mathrm{Pr}_2C_6H_3)\}_2]M[(\mu\text{-}O)Si(OtBu)_2(OH)]_2$ (M = Al (**1**), Ga (**2**)) molecular disilicates.

■ EXPERIMENTAL SECTION

General Considerations. All manipulations described below were performed under a dried nitrogen atmosphere using Schlenk and glovebox techniques. The solvents were purchased from Aldrich and dried prior to use with an MBraun Solvent Purification System using Grubs' type columns. $M'(NR_2)_4$ (M′ = Ti, Zr, R = Me; M′ = Hf, R = Et) were purchased from Aldrich and used as received, whereas $(tBuO)_2Si(OH)_2$,[13] $[HC\{C(Me)N(2,6\text{-}i\mathrm{Pr}_2C_6H_3)\}_2]AlH_2$,[14a] $[HC\{C(Me)N(2,6\text{-}i\mathrm{Pr}_2C_6H_3)\}_2]Ga(NHEt)_2$,[14b] $Ti(NEt_2)_4$,[14c] and $Zr(NEt_2)_4$[14c] were prepared according to literature procedures. C_6D_6 and tol-d_8 were distilled from Na/K alloy and degassed before use. NMR spectroscopic data were recorded either on a Varian NMRSystem 500 MHz, Bruker Avance III 400 MHz, or Bruker Avance III 300 MHz spectrometer and referenced to residual protons of the deuterated solvent. Mass spectrometry for compounds **3**−**11** was futile due to poor ionization of the molecules (ESI) or because the molecular mass of the compounds lies outside the detection limits of the available equipment (EI).[15] Therefore, mass spectra of compounds **3**−**11** are not reported. Elemental analyses (C, H, N) were carried out either on a VarioMICRO cube analyzer or in Galbraith Laboratories Inc. (Knoxville, TN). Dried monocrystals were used for these analyses for all compounds. All samples were prepared in a glovebox and kept under a nitrogen atmosphere prior to the analysis. The high reactivity of the compounds, varying content of solvents, and possible formation of silicon and aluminum carbides during the combustion are responsible for the observed differences between the theoretical and experimental values. ^1H NMR spectra of compounds **3**−**11** at room temperature (25 °C) are too broad to be assigned; thus, ^1H NMR spectra are reported at 0 or −10 °C. Even at low temperatures, it is not possible to accurately determine the coupling constants (J_{H-H}) of some signals. Therefore, these are not reported. Similarly, ^{13}C and ^{29}Si NMR spectra are not reported because of very broad signals due to conformational changes (*vide infra*). Selected ^1H NMR spectra for compounds **3**−**11** can be found in the Supporting Information. The IR spectra were measured on Bruker Tensor 27 or Bruker Alpha.

X-ray Crystallography. Single crystals were mounted either on a Bruker Smart Apex (Apex 1k detector) or a Bruker APEX DUO diffractometer equipped with an Apex II CCD detector at 100 K. Frames were collected using ω scans and integrated with SAINT.[16] Multiscan absorption correction (SADABS)[16] was applied. The structures were solved by direct methods (SHELXS)[17] and refined using full-matrix least-squares on F^2 with SHELXL-97[17] using the SHELXLE GUI.[18] Weighted R factors, R_w, and all goodness-of-fit indicators, are based on F^2. All non-hydrogen atoms were refined anisotropically. The hydrogen atoms of the C−H bonds were placed in idealized positions, whereas the hydrogen atoms from the OH moieties were localized from the difference electron density map and their position was refined with U_{iso} tied to the parent atom with distance restraints. The disordered groups and solvent molecules (**1** 1 × O*t*Bu, 2 × *t*Bu; **2** 1 × O*t*Bu, 1 × *t*Bu; **6** 1 × *i*Pr; **7** 1 × *i*Pr, 2.73 × toluene; **8** 2.88 × toluene; **9** 1 × O*t*Bu, 1.5 toluene + hexane; **10** 2.83 × toluene; **11** 1 × O*t*Bu, 1.5 hexane + toluene) were refined using geometry (SADI, SAME, FLAT) and U_{ij} restraints (SIMU, DELU, ISOR) implemented in SHELXL-97.[15] The OH distances in **1** and **2** were restrained using DFIX.

Details for $[HC\{C(Me)N(2,6\text{-}i\mathrm{Pr}_2C_6H_3)\}_2]Al[(\mu\text{-}O)Si(OH)(OtBu)]_2$ (**1**) follow: A solution of $(tBuO)_2Si(OH)_2$ (0.54 g, 2.59 mmol) in THF (10 mL) was slowly added to a stirred solution of $[HC\{C(Me)N(2,6\text{-}i\mathrm{Pr}_2C_6H_3)\}_2]AlH_2$ (0.50 g, 1.12 mmol) in THF (30 mL) at −108 °C. After reaching room temperature, the reaction was stirred for 6 h giving a colorless solution. The solvent was removed and the product crystallized from toluene as transparent crystals. Yield: 0.79 g (76%). Mp 163 °C (dec). Anal. (%) Calcd for $C_{45}H_{79}AlN_2O_8Si_2$ (859.27 g mol^{-1}): C 62.90, H 9.27, N 3.26. Found: C 62.97, H 9.28, N 3.28. FT-IR (KBr pellet) $\tilde{\nu}$/cm^{-1}: 3620, 3505 (w, br, ν O−H). EI-MS: *m*/*z* (%) 859(31) $[M]^+$, 41(100) $[C_3H_5]^+$. ^1H NMR (400 MHz, C_6D_6, 20 °C): δ = 1.22 (d, 12 H, $^3J_{H-H}$ = 6.8 Hz, $CH(CH_3)_2$), 1.30 (s, 36 H, $C(CH_3)_3$), 1.53 (s, 6 H, CH_3), 1.53 (d, 12 H, $^3J_{H-H}$ = 6.8 Hz, $CH(CH_3)_2$), 3.04 (s, 2 H, O*H*), 3.47 (sept, 4 H, $^3J_{H-H}$ = 6.8 Hz, $CH(CH_3)_2$), 4.97 (s, 1 H, γ-*H*), 7.19 ppm (m, 6 H, *H* of Ar). $^{13}C\{^1H\}$ NMR (75.43 MHz, C_6D_6, 20 °C): δ = 24.1 (CH_3), 25.4 ($CH(CH_3)_2$), 26.3 ($CH(CH_3)_2$), 28.7 ($CH(CH_3)_2$), 31.9 ($C(CH_3)_3$), 72.2 ($C(CH_3)_3$), 99.2 (γ-*C*), 125.1, 127.6, 141.2, 145.0 (*C* of Ar), 171.8 ppm (*C*=N). $^{29}Si\{^1H\}$ NMR (99.33 MHz, C_6D_6, 20 °C): δ = −97 ppm ($O_2Si(OtBu)_2$).

Details for $[HC\{C(Me)N(2,6\text{-}i\mathrm{Pr}_2C_6H_3)\}_2]Ga[(\mu\text{-}O)Si(OH)(OtBu)]_2$ (**2**) follow: A solution of $(tBuO)_2Si(OH)_2$ (0.40 g, 1.80 mmol) in THF (10 mL) was slowly added to a stirred thawing solution of $[HC\{C(Me)N(2,6\text{-}i\mathrm{Pr}_2C_6H_3)\}_2]Ga(NHEt)_2$ (0.50 g, 0.90 mmol) in THF (30 mL). The reaction mixture was allowed to reach room temperature and stirred for 2 h giving a transparent solution. The solvent was removed and the product crystallized from hexane as colorless crystals. Yield: 0.51 g (65%). Mp 135 °C. Anal. (%) Calcd for $C_{45}H_{79}GaN_2O_8Si_2$ (902.01 g mol^{-1}): C 59.92, H 8.83, N 3.11. Found: C 60.2, H 8.9, N 3.2. FT-IR (ATR) $\tilde{\nu}$/cm^{-1}: 3690, 3509 (w, br, ν O−H). EI-MS: *m*/*z* (%) 900(5) $[M]^+$, 692(32) $[M{-}(OH)_2Si(OtBu)_2]^+$, 41(100) $[C_3H_5]^+$. ^1H NMR (500 MHz, C_6D_6, 20 °C): δ = 1.21 (d, 6H, $^3J_{H-H}$ = 6.8 Hz, $CH(CH_3)_2$), 1.31 (s, 18H, $(CH_3)_3COSi$), 1.50 (s, 6 H, CH_3), 1.55 (d, 6H, $^3J_{H-H}$ = 6.8 Hz, $CH(CH_3)_2$), 3.42 (s, 2H, SiO*H*), 3.48 (sept, 4H, $^3J_{H-H}$ = 6.8 Hz, $CH(CH_3)_2$), 4.80 (s, 1H, γ-C*H*), 7.10−7.25 ppm (m, 6H, *H* of Ar). $^{13}C\{^1H\}$ NMR (75.43 MHz, C_6D_6, 25 °C): δ = 24.0 (CH_3), 25.0 ($CH(CH_3)_2$), 25.8 ($CH(CH_3)_2$), 28.3 ($CH(CH_3)_2$), 31.5 ($C(CH_3)_2$), 71.9 ($C(CH_3)_3$), 97.0 (γ-*C*H), 124.6, 127.6, 140.6, 144.6 (*C* of Ar), 171.3 (*C*=N) ppm. $^{29}Si\{^1H\}$ NMR (99.33 MHz, C_6D_6, 20 °C): δ = −94 ppm ($O_2Si(OtBu)_2$).

Details for $[HC\{C(Me)N(2,6\text{-}i\mathrm{Pr}_2C_6H_3)\}_2]Al[(\mu\text{-}O)Si(\mu\text{-}O)(OtBu)_2]_2M'(NEt_2)_2$ (**3** M′ = Zr; **5** M′ = Hf) follow: A solution of **1** (0.30 g, 0.35 mmol) in toluene (15 mL) was added dropwise to a stirred solution of $Zr(NEt_2)_4$ (0.14 g, 0.38 mmol) for **3** or $Hf(NEt_2)_4$ (0.18 g, 0.38 mmol) for **5**, respectively, in toluene (30 mL) at −78 °C.

The reaction mixture was allowed to reach room temperature and stirred for additional 12 h resulting in a clear solution. After removing all volatiles, the crude product was crystallized from toluene at −30 °C.

Details for [HC{C(Me)N(2,6-*i*Pr$_2$C$_6$H$_3$)}$_2$]Ga[(μ-O)Si(μ-O)(O*t*Bu)$_2$]$_2$M′(NEt$_2$)$_2$ (**4** M′ = Zr; **6** M′ = Hf) follow: A solution of **2** (0.20 g, 0.22 mmol) in THF (10 mL) was added dropwise to a thawing solution of Zr(NEt$_2$)$_4$ (0.09 g, 0.24 mmol) for **4** or Hf(NEt$_2$)$_4$ (0.10 g, 0.24 mmol) for **6**, in THF (10 mL). The reaction mixture was allowed to reach room temperature and stirred for 2 h resulting in a clear slightly yellow solution. After removing all volatiles, the crude product was crystallized from hexane at −30 °C.

Details for [HC{C(Me)N(2,6-*i*Pr$_2$C$_6$H$_3$)}$_2$]Al[(μ-O)Si(μ-O)(O*t*Bu)$_2$]$_2$Zr(NEt$_2$)$_2$ (**3**) follow: White crystals. Yield: 0.28 g (74%). Mp 273 − 275 °C (dec). Anal. (%) Calcd for $C_{53}H_{97}AlN_4O_8Si_2Zr$ (1092.74 g mol^{-1}): C 58.25, H 8.95, N 5.13. Found: C 57.87, H 8.92, N 5.00. ^{1}H NMR (500 MHz, toluene-d_8, 0 °C): δ = 1.07 (s, 18 H, C(C*H*$_3$)$_3$), 1.10 (d, 6 H, $^3J_{\mathrm{H-H}}$ = 6.8 Hz, CH(C*H*$_3$)$_2$), 1.24 (t, 12 H, $^3J_{\mathrm{H-H}}$ = 6.8 NCH$_2$C*H*$_3$), 1.43 (d, 6 H, $^3J_{\mathrm{H-H}}$ = 6.5 Hz, CH(C*H*$_3$)$_2$), 1.47 (d, 6 H, $^3J_{\mathrm{H-H}}$ = 6.8 Hz, CH(C*H*$_3$)$_2$), 1.54 (s, 6 H, C*H*$_3$), 1.58 (s, 18 H, C(C*H*$_3$)$_3$), 1.62 (d, 6 H, $^3J_{\mathrm{H-H}}$ = 6.5 Hz, CH(C*H*$_3$)$_2$), 3.18 (dq, 4 H, $^2J_{\mathrm{H-H}}$ = 13.8 Hz, $^3J_{\mathrm{H-H}}$ = 6.8 Hz, NC*H*$_2$CH$_3$), 3.28 (sept, 2 H, $^3J_{\mathrm{H-H}}$ = 6.8 Hz, C*H*(CH$_3$)$_2$), 3.34 (dq, 4 H, $^2J_{\mathrm{H-H}}$ = 13.8 Hz, $^3J_{\mathrm{H-H}}$ = 6.8 Hz, NC*H*$_2$CH$_3$), 3.84 (sept, 2 H, $^3J_{\mathrm{H-H}}$ = 6.5 Hz, C*H*(CH$_3$)$_2$), 5.05 (s, 1 H, γ-*H*), 7.12−7.20 ppm (m, 6 H, *H* of Ar).

Details for [HC{C(Me)N(2,6-*i*Pr$_2$C$_6$H$_3$)}$_2$]Ga[(μ-O)Si(μ-O)(O*t*Bu)$_2$]$_2$Zr(NEt$_2$)$_2$ (**4**) follow: White crystals. Yield: 0.11 g (44%). Mp 236−237 °C. Anal. (%) Calcd for $C_{53}H_{97}GaN_4O_8Si_2Zr$ (1092.74 g mol^{-1}): C 56.05, H 8.62, N 4.94. Found: C 56.47, H 8.32, N 4.66). ^{1}H NMR (500 MHz, toluene-d_8, − 10 °C): δ = 0.90 (t, 12 H, $^3J_{\mathrm{H-H}}$ = 7.0 Hz, NCH$_2$C*H*$_3$), 0.97 (s, 18 H, C(C*H*$_3$)$_3$), 1.05 (d, 6 H, br, CH(C*H*$_3$)$_2$), 1.07 (d, 6 H, br, CH(C*H*$_3$)$_2$), 1.28 (s, 6 H, C*H*$_3$), 1.44 (s, 18 H, C(C*H*$_3$)$_3$), 1.52 (d, 6 H, $^3J_{\mathrm{H-H}}$ = 7.0 Hz, CH(C*H*$_3$)$_2$), 1.61 (d, 6 H, $^3J_{\mathrm{H-H}}$ = 6.5 Hz, CH(C*H*$_3$)$_2$), 3.22 (dq, 4 H, br, NC*H*$_2$CH$_3$), 3.43 (dq, 4 H, br, NC*H*$_2$CH$_3$), 3.62 (sept, 4 H, br, C*H*(CH$_3$)$_2$), 4.77 (s, 1 H, γ-*H*), 7.02−7.40 ppm (m, 6 H, *H* of Ar).

Details for [HC{C(Me)N(2,6-*i*Pr$_2$C$_6$H$_3$)}$_2$]Al[(μ-O)Si(μ-O)(O*t*Bu)$_2$]$_2$Hf(NEt$_2$)$_2$ (**5**) follow: White crystals. Yield: 0.30 g (73%). Mp 269−271 °C (dec). Anal. (%) Calcd for $C_{53}H_{97}AlN_4O_8Si_2Hf$ (1180.61 g mol^{-1}): C 53.95, H 8.29, N 4.75. Found: C 53.08, H 8.20, N 4.52. ^{1}H NMR (500 MHz, toluene-d_8, − 10 °C): δ = 1.08 (s, 18 H, C(C*H*$_3$)$_3$), 1.10 (d, 6 H, $^3J_{\mathrm{H-H}}$ = 7.0 Hz, CH(C*H*$_3$)$_2$), 1.24 (t, 12 H, $^3J_{\mathrm{H-H}}$ = 6.5 Hz, NCH$_2$C*H*$_3$), 1.43 (d, 6 H, $^3J_{\mathrm{H-H}}$ = 7.0 Hz, CH(C*H*$_3$)$_2$), 1.47 (d, 6 H, $^3J_{\mathrm{H-H}}$ = 6.5 Hz, CH(C*H*$_3$)$_2$), 1.53 (s, 6 H, C*H*$_3$), 1.58 (s, 18 H, C(C*H*$_3$)$_3$), 1.63 (d, 6 H, $^3J_{\mathrm{H-H}}$ = 6.5 Hz, CH(C*H*$_3$)$_2$), 3.26 (br, 4 H, NC*H*$_2$CH$_3$), 3.26 (sept, 2 H, $^3J_{\mathrm{H-H}}$ = 7.0 Hz, C*H*(CH$_3$)$_2$), 3.36 (br, 4 H, NC*H*$_2$CH$_3$), 3.82 (sept, 2 H, $^3J_{\mathrm{H-H}}$ = 6.5 Hz, C*H*(CH$_3$)$_2$), 5.04 (s, 1 H, γ-*H*), 7.13−7.18 ppm (m, 6 H, *H* of Ar).

Details for [HC{C(Me)N(2,6-*i*Pr$_2$C$_6$H$_3$)}$_2$]Ga[(μ-O)Si(μ-O)(O*t*Bu)$_2$]$_2$Hf(NEt$_2$)$_2$ (**6**) follow: White crystals. Yield: 0.28 g (74%). Mp 273−275 °C (dec). Anal. (%) Calcd for $C_{53}H_{97}AlN_4O_8Si_2Hf$ (1221.89 g mol^{-1}): C 52.05, H 8.00, N 4.58. Found: C 52.45, H 8.20, N 4.12. ^{1}H NMR (500 MHz, toluene-d_8, −10 °C): δ = 1.07 (s, 18 H, C(C*H*$_3$)$_3$), 1.09 (d, 6 H, $^3J_{\mathrm{H-H}}$ = 6.8 Hz, CH(C*H*$_3$)$_2$), 1.23 (t, 12 H, $^3J_{\mathrm{H-H}}$ = 6.8 Hz, NCH$_2$C*H*$_3$), 1.42 (d, 6 H, $^3J_{\mathrm{H-H}}$ = 6.8 Hz, CH(C*H*$_3$)$_2$), 1.47 (d, 6 H, $^3J_{\mathrm{H-H}}$ = 6.8 Hz, CH(C*H*$_3$)$_2$), 1.52 (s, 6 H, C*H*$_3$), 1.56 (s, 18 H, C(C*H*$_3$)$_3$), 1.61 (d, 6 H, $^3J_{\mathrm{H-H}}$ = 6.8 Hz, CH(C*H*$_3$)$_2$), 3.17 (dq, 4 H, $^2J_{\mathrm{H-H}}$ = 13.4 Hz, $^3J_{\mathrm{H-H}}$ = 6.8 Hz, NC*H*$_2$CH$_3$), 3.27 (sept, 2 H, $^3J_{\mathrm{H-H}}$ = 6.8 Hz, C*H*(CH$_3$)$_2$), 3.33 (dq, 4 H, br, NC*H*$_2$CH$_3$), 3.83 (sept, 2 H, $^3J_{\mathrm{H-H}}$ = 6.8 Hz, C*H*(CH$_3$)$_2$), 5.03 (s, 1 H, γ-*H*), 7.02−7.18 ppm (m, 6 H, *H* of Ar).

Details for {[HC{C(Me)N(2,6-*i*Pr$_2$C$_6$H$_3$)}$_2$]Al[(μ-O)Si(μ-O)(O*t*Bu)$_2$]$_2$}$_2$M (**7** M = Ti, **8** M = Zr, **10** M = Hf) follow: A solution of Ti(NMe$_2$)$_4$ (0.05 g, 0.23 mmol) for **7**, Zr(NMe$_2$)$_4$ (0.06 g, 0.23 mmol) for **8**, or Hf(NEt$_2$)$_4$ (0.11 g, 0.23 mmol) for **10**, respectively, in toluene (10 mL) was added dropwise to a stirred solution of [HC{C(Me)N(2,6-*i*Pr$_2$C$_6$H$_3$)}$_2$]Al[(μ-O)Si(OH)(O*t*Bu)$_2$]$_2$ (**1**) (0.40 g, 0.46 mmol) in toluene (30 mL) at −78 °C. The reaction mixture was allowed to slowly warm to room temperature and stirred for 16 h, resulting in a slightly yellow solution. After removing all volatiles the crude product was crystallized from toluene at −30 °C.

Details for {[HC{C(Me)N(2,6-*i*Pr$_2$C$_6$H$_3$)}$_2$]Ga[(μ-O)Si(μ-O)(O*t*Bu)$_2$]$_2$}$_2$M (**9** M = Zr, **11** M = Hf) follow: A solution of Zr(NMe$_2$)$_4$ (0.03 g, 0.11 mmol) for **9** or Hf(NEt$_2$)$_4$ (0.04 g, 0.10 mmol) for **11**, in THF (10 mL), was added dropwise to a thawing solution of [HC{C(Me)N(2,6-*i*Pr$_2$C$_6$H$_3$)}$_2$]Ga[(μ-O)Si(OH)(O*t*Bu)$_2$]$_2$ (**2**) (0.20 g, 0.22 mmol) in THF (30 mL). The reaction mixture was allowed to slowly warm to room temperature and stirred for additional 4 h, resulting in slightly yellow solutions. After removing all volatiles, the crude product was crystallized from hexane at −30 °C.

Details for {[HC{C(Me)N(2,6-*i*Pr$_2$C$_6$H$_3$)}$_2$]Al[(μ-O)Si(μ-O)(O*t*Bu)$_2$]$_2$}$_2$Ti (**7**) follow: White crystals. Yield: 0.27 g (66%). Mp 126 °C (dec). Anal. (%) Calcd for $C_{90}H_{154}Al_2N_4O_{16}Si_4Ti$ (1762.38 g mol^{-1}): C 61.34, H 8.81, N 3.18. Found: C 61.87, H 8.77, N 3.03. ^{1}H NMR (500 MHz, toluene-d_8, − 10 °C): δ = 1.00 (s, 18 H, C(C*H*$_3$)$_3$), 1.02 (d, 6 H, $^3J_{\mathrm{H-H}}$ = 6.5 Hz, CH(C*H*$_3$)$_2$), 1.07 (d, 6 H, $^3J_{\mathrm{H-H}}$ = 6.5 Hz, CH(C*H*$_3$)$_2$), 1.30 (d, 6 H, $^3J_{\mathrm{H-H}}$ = 6.5 Hz, CH(C*H*$_3$)$_2$), 1.31 (s, 18 H, C(C*H*$_3$)$_3$), 1.44 (s, 6 H, C*H*$_3$), 1.48 (s, 18 H, C(C*H*$_3$)$_3$), 1.48 (s, 6 H, br, CH(C*H*$_3$)$_2$), 1.52 (d, 6 H, $^3J_{\mathrm{H-H}}$ = 7.0 Hz, CH(C*H*$_3$)$_2$), 1.58 (s, 6 H, C*H*$_3$), 1.61 (d, 6 H, $^3J_{\mathrm{H-H}}$ = 7.0 Hz, CH(C*H*$_3$)$_2$), 1.63 (d, 6 H, $^3J_{\mathrm{H-H}}$ = 7.0 Hz, CH(C*H*$_3$)$_2$), 1.68 (s, 18 H, C(C*H*$_3$)$_3$), 1.91 (d, 6 H, $^3J_{\mathrm{H-H}}$ = 6.5 Hz, CH(C*H*$_3$)$_2$), 3.24 (sept, 2 H, $^3J_{\mathrm{H-H}}$ = 6.5 Hz, C*H*(CH$_3$)$_2$), 3.40 (sept, 2 H, $^3J_{\mathrm{H-H}}$ = 6.5 Hz, C*H*(CH$_3$)$_2$), 3.55 (sept, 2 H, $^3J_{\mathrm{H-H}}$ = 7.0 Hz, C*H*(CH$_3$)$_2$), 3.69 (sept, 2 H, $^3J_{\mathrm{H-H}}$ = 7.0 Hz, C*H*(CH$_3$)$_2$), 4.93 (s, 2 H, γ-*H*), 7.14−7.42 ppm (m, 12 H, *H* of Ar).

Details for {[HC{C(Me)N(2,6-*i*Pr$_2$C$_6$H$_3$)}$_2$]Al[(μ-O)Si(μ-O)(O*t*Bu)$_2$]$_2$}$_2$Zr (**8**) follow: White crystals. Yield: 0.28 g (68%). Mp 121 °C (dec). Anal. (%) Calcd for $C_{90}H_{154}Al_2N_4O_{16}Si_4Zr$ (1805.73 g mol^{-1}): C 59.86, H 8.60, N 3.10. Found: C 59.51, H 8.70, N 2.88. ^{1}H NMR (500 MHz, toluene-d_8, − 10 °C): δ = 1.00 (s, 18 H, C(C*H*$_3$)$_3$), 1.08 (s, 12 H, br, CH(C*H*$_3$)$_2$), 1.21 (s, 18 H, C(C*H*$_3$)$_3$), 1.37 (d, 6 H, $^3J_{\mathrm{H-H}}$ = 6.5 Hz, CH(C*H*$_3$)$_2$), 1.48 (s, 6 H, C*H*$_3$), 1.48 (s, 6 H, br, CH(C*H*$_3$)$_2$), 1.53 (s, 12 H, br, CH(C*H*$_3$)$_2$), 1.53 (s, 18 H, C(C*H*$_3$)$_3$), 1.59 (s, 6 H, C*H*$_3$), 1.63 (d, 12 H, $^3J_{\mathrm{H-H}}$ = 6.5 Hz, CH(C*H*$_3$)$_2$), 1.67 (s, 18 H, C(C*H*$_3$)$_3$), 1.83 (d, 6 H, $^3J_{\mathrm{H-H}}$ = 6.5 Hz, CH(C*H*$_3$)$_2$), 3.21 (sept, 2 H, $^3J_{\mathrm{H-H}}$ = 6.5 Hz, C*H*(CH$_3$)$_2$), 3.37 (sept, 2 H, br, C*H*(CH$_3$)$_2$), 3.72 (sept, 4 H, br, C*H*(CH$_3$)$_2$), 5.00 (s, 2 H, γ-*H*), 7.14−7.31 ppm (m, 12 H, *H* of Ar).

Details for {[HC{C(Me)N(2,6-*i*Pr$_2$C$_6$H$_3$)}$_2$]Ga[(μ-O)Si(μ-O)(O*t*Bu)$_2$]$_2$}$_2$Zr (**9**) follow: White crystals. Yield: 0.14 g (68%). Mp > 400 °C. Anal. (%) Calcd for $C_{90}H_{154}Ga_2N_4O_{16}Si_4Zr$ (1889.71 g mol^{-1}): C 57.15, H 8.21, N 2.96. Found: C 55.51, H 7.92, N 2.55. ^{1}H NMR (500 MHz, toluene-d_8, − 10 °C): δ = 0.99 (s, 18 H, C(C*H*$_3$)$_3$), 1.02 (d, 6 H, $^3J_{\mathrm{H-H}}$ = 6.6 Hz, CH(C*H*$_3$)$_2$), 1.08 (d, 6 H, $^3J_{\mathrm{H-H}}$ = 6.6 Hz, CH(C*H*$_3$)$_2$), 1.30 (d, 6 H, br, CH(C*H*$_3$)$_2$), 1.31 (s, 18 H, C(C*H*$_3$)$_3$), 1.44 (s, 6 H, C*H*$_3$), 1.48 (s, 18 H, C(C*H*$_3$)$_3$), 1.52 (d, 6 H, br, CH(C*H*$_3$)$_2$), 1.58 (s, 6 H, C*H*$_3$), 1.62 (d, 12 H, br, CH(C*H*$_3$)$_2$), 1.63 (d, 6 H, br, CH(C*H*$_3$)$_2$), 1.69 (s, 18 H, C(C*H*$_3$)$_3$), 1.90 (d, 6 H, $^3J_{\mathrm{H-H}}$ = 6.8 Hz, CH(C*H*$_3$)$_2$), 3.24 (sept, 2 H, $^3J_{\mathrm{H-H}}$ = 6.8 Hz, C*H*(CH$_3$)$_2$), 3.39 (sept, 2 H, $^3J_{\mathrm{H-H}}$ = 6.6 Hz, C*H*(CH$_3$)$_2$), 3.54 (sept, 2 H, $^3J_{\mathrm{H-H}}$ = 6.5 Hz, C*H*(CH$_3$)$_2$), 3.69 (sept, 2 H, $^3J_{\mathrm{H-H}}$ = 6.5 Hz, C*H*(CH$_3$)$_2$), 4.93 (s, 2 H, γ-*H*), 7.18−7.42 ppm (m, 12 H, *H* of Ar).

Details for {[HC{C(Me)N(2,6-*i*Pr$_2$C$_6$H$_3$)}$_2$]Al[(μ-O)Si(μ-O)(O*t*Bu)$_2$]$_2$}$_2$Hf (**10**) follow: White crystals. Yield: 0.25 g (58%). Mp 132 °C (dec). Anal. (%) Calcd for $C_{90}H_{154}Al_2N_4O_{16}Si_4Hf$ (1893.00 g mol^{-1}): C 57.10, H 8.20, N 2.96. Found: C 57.11, H 8.34, N 2.83. ^{1}H NMR (500 MHz, toluene-d_8, − 10 °C): δ = 1.00 (s, 18 H, C(C*H*$_3$)$_3$), 1.07 (d, 6 H, br, CH(C*H*$_3$)$_2$), 1.08 (d, 6 H, $^3J_{\mathrm{H-H}}$ = 6.25 Hz, CH(C*H*$_3$)$_2$), 1.22 (s, 18 H, C(C*H*$_3$)$_3$), 1.37 (d, 6 H, $^3J_{\mathrm{H-H}}$ = 6.25 Hz, CH(C*H*$_3$)$_2$), 1.48 (s, 6 H, C*H*$_3$), 1.48 (s, 6 H, br, CH(C*H*$_3$)$_2$), 1.53 (s, 12 H, br, CH(C*H*$_3$)$_2$), 1.53 (s, 18 H, C(C*H*$_3$)$_3$), 1.59 (s, 6 H, C*H*$_3$), 1.63 (d, 12 H, $^3J_{\mathrm{H-H}}$ = 7.5 Hz, CH(C*H*$_3$)$_2$), 1.67 (s, 18 H, C(C*H*$_3$)$_3$), 1.82 (d, 6 H, $^3J_{\mathrm{H-H}}$ = 7.5 Hz, CH(C*H*$_3$)$_2$), 3.21 (sept, 2 H, $^3J_{\mathrm{H-H}}$ = 6.25 Hz, C*H*(CH$_3$)$_2$), 3.36 (sept, 2 H, $^3J_{\mathrm{H-H}}$ = 6.25 Hz, C*H*(CH$_3$)$_2$), 3.71 (sept, 4 H, br, C*H*(CH$_3$)$_2$), 5.01 (s, 2 H, γ-*H*), 7.14−7.30 ppm (m, 12 H, *H* of Ar).

Details for {[HC{C(Me)N(2,6-*i*Pr$_2$C$_6$H$_3$)}$_2$]Ga[(μ-O)Si(μ-O)(O*t*Bu)$_2$]$_2$}$_2$Hf (**11**) follow: White crystals. Yield: 0.15 g (70%). Mp

> 400 °C. Anal. (%) Calcd for $C_{90}H_{154}Ga_2N_4O_{16}Si_4Hf$ (1976.98 g mol^{-1}): C 54.63, H 7.85, N 2.83. Found: C 54.51, H 7.62, N 2.50. ^{1}H NMR (500 MHz, toluene-d_8, − 10 °C): δ = 1.12 (s, 18 H, C(CH_3)$_3$), 1.17 (d, 6 H, br, CH(CH_3)$_2$), 1.19 (d, 6 H, br, CH(CH_3)$_2$), 1.20 (d, 6 H, br, CH(CH_3)$_2$, 1.37 (d, 6 H, br, CH(CH_3)$_2$), 1.49 (s, 6 H, CH_3), 1.57 (s, 6 H, br, CH(CH_3)$_2$), 1.53 (s, 12 H, br, CH(CH_3)$_2$), 1.62 (d, 12 H, br, CH(CH_3)$_2$), 1.67 (s, 18 H, C(CH_3)$_3$), 3.15 (sept, 2 H, br, CH(CH_3)$_2$), 3.27 (sept, 2 H, br, CH(CH_3)$_2$), 3.33 (sept, 4 H, br, CH(CH_3)$_2$), 3.76 (sept, 4 H, br, CH(CH_3)$_2$), 4.81 (s, 2 H, *γ-H*), 7.05−7.16 ppm (m, 12 H, *H* of Ar).

■ RESULTS AND DISCUSSION

The synthesis of **1** and **2** represents a major challenge due the reduced control over the kinetic and thermodynamic factors involved in its isolation. Compared to **a** and **b** (Figure 1), where the formation of the SiO_2M rings is hampered due the high steric bulk of the ligand [HC{C(Me)N(2,6-*i*Pr$_2$C$_6$H$_3$)}$_2$]$^-$ and its high ring strain, the substitution of the M−OH group for a highly reactive M−O−Si−OH substituent reduces this steric control over the condensation of the terminal −OH groups and, therefore, over the formation of the six-membered Si−O−Si−O−M−O ring.[19] To suppress this condensation, the reactions between [HC{C(Me)N(2,6-*i*Pr$_2$C$_6$H$_3$)}$_2$]AlH$_2$ or [HC{C(Me)N(2,6-*i*Pr$_2$C$_6$H$_3$)}$_2$]Ga(NHEt)$_2$ and 2 equiv of (tBuO)$_2$Si(OH)$_2$ were performed at low temperature. The slow addition of the silanediol and relatively short reaction times resulted in a clean formation of the alumo- and gallodisilicates [HC{C(Me)N(2,6-*i*Pr$_2$C$_6$H$_3$)}$_2$]M[(μ-O)Si(OH)(O*t*Bu)$_2$]$_2$ (M = Al (**1**), Ga (**2**)) in high yields as white crystalline solids (Scheme 1). The compounds are highly soluble in organic solvents, display similar spectroscopic characteristics, are thermally stable up to 135 °C, and can be stored in a crystalline form for several months under an inert atmosphere. However, slow decomposition occurs in solution after 24 h, and it is likely caused by the condensation of the silanol groups with the concomitant loss of water (*vide infra*).

Scheme 1. Synthesis of Disilicates 1 and 2

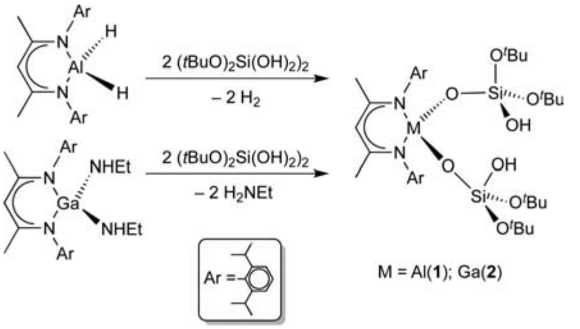

The solid state IR spectra of compounds **1** and **2** show two different bands for two nonequivalent Si−OH moieties ($\tilde{\nu}$ = 3620, 3505 for **1** and 3690, 3509 for **2** cm^{-1}), with the broader lower energy vibration band, indicating the formation of a hydrogen bond. The presence of two different OH groups and one hydrogen bond in the solid state was confirmed by X-ray diffraction studies and will be discussed later. On the other hand, NMR studies reveal different behavior in solution. Through ^{1}H NMR spectroscopy it is possible to observe a signal pattern for the hydrocarbon backbone of the ligand that corresponds to a C_{2v} symmetry. This symmetry is characteristic for two equivalent substituents attached to the M center in the [HC{C(Me)N(2,6-*i*Pr$_2$C$_6$H$_3$)}$_2$]MX$_2$ systems. Furthermore, ^{1}H NMR spectra of **1** and **2** are devoid of the hydride or NHEt signals, but signals for the (tBuO)$_2$Si (δ 1.30 (**1**), 1.31 ppm (**2**)) and for the Si−OH groups (δ 3.04 (**1**), 3.45 ppm (**2**)) are present. The singlets at δ −97 (**1**), −94 ppm (**2**) in the ^{29}Si{^{1}H} NMR spectra confirmed the presence of two equivalent silicate substituents attached to the metal atom. This clearly shows that the hydrogen bond between the silicate groups is not strong enough to persist in solution and, consequently, the free movement of these groups is responsible for the slow decomposition of **1** and **2** in solution via condensation of the OH groups. Unfortunately, despite all our efforts, we have not been able to elucidate the decomposition pathway of **1** and **2**, and thus, the only identified decomposition product corresponds to the ligand [HC{C(Me)N(2,6-*i*Pr$_2$C$_6$H$_3$)}$_2$]H.

Single crystals of the disilicates **1** and **2** were grown from saturated toluene (**1**) or hexane (**2**) solutions at −30 °C. Compounds **1** and **2** are isomorphous and crystallize in the monoclinic space group $P2_1/n$ with one molecule of the disilicate in the asymmetric unit (Figure 2). The solid-state structures of both compounds present characteristics features analogous to those observed in **a** and **b**. Compounds **1** and **2** feature a highly distorted tetrahedral geometry for the Al or Ga atoms, as a result of the reduced bite angle of the ligand [HC{C(Me)N(2,6-*i*Pr$_2$C$_6$H$_3$)}$_2$]$^-$ [N−M−N 98.6(1)° (**1**), 99.2(1)° (**2**)].

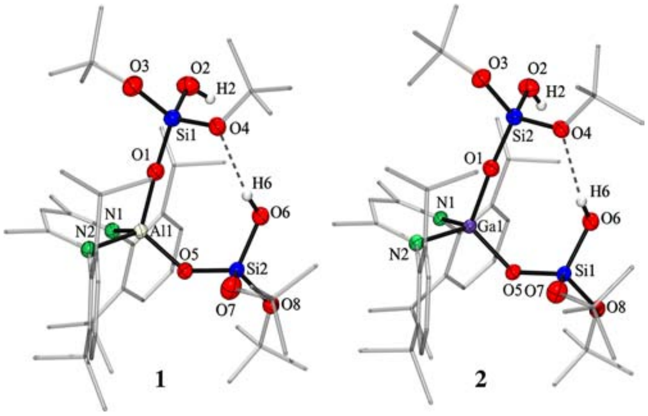

Figure 2. Molecular structures of **1** and **2**. Carbon ellipsoids and carbon-bound hydrogen atoms have been omitted for clarity. Thermal ellipsoids of noncarbon atoms are set at 50% probability level.

The M−O bond distances reflect the size and the acidity of the metals and are shorter for the aluminum atom in **1** (1.701(2), 1.715(1) Å) than for the gallium atom in **2** (1.782(1), 1.801(1) Å), but analogous to **a** (1.711(1) Å) and **b** (1.800(1) Å), respectively. The SiO$_4$ moieties in compounds **1** and **2** are similar, and all the Si atoms exhibit a higher distorted tetrahedral geometry as can be seen from the values for the O−Si−O angles [103.9(3)−113.5(8) ° (**1**), 102.7(1)−114.5(1) ° (**2**)]. The Si−O bond lengths in **1** (1.586(2)−1.640(2) Å) and in **2** (1.582(1)−1.638(1) Å) are identical; however, they feature large variations. Table 1 contains selected distances and angles for compounds **1** and **2**, whereas the crystallographic details are summarized in Table 2. The molecular structures also confirm the formation of an intramolecular hydrogen bond between one Si−OH group and an oxygen atom from a O*t*Bu group from the second silicate moiety with a O···O distance of 2.972(2) Å (**1**) and 2.954(2) Å (**2**). These distances are slightly longer

Table 1. Selected Bond Lengths [Å] and Angles [deg] for Compounds 1 and 2

	1[c]	**2**[d]
M–O(Si)	1.701(2)	1.782(1)
	1.715(2)	1.801(1)
M–N	1.890(2)	1.919(2)
	1.892(2)	1.932(2)
Si–O(M)	1.586(2)	1.582(1)
	1.607(2)	1.606(1)
Si–O(H)	1.630(2)	1.638(2)
	1.640(2)	1.628(1)
Si–O(*t*Bu)[a]	1.616(2)	1.626(3)
O–M–O	113.2(1)	113.1(1)
N–M–N	98.6(1)	99.2(1)
O–Si–O[b]	105.8(1)–113.3(1)	105.5(1)–114.6(1)
	103.9(3)–113.5(8)	102.7(1)–114.5(9)
M–O–Si	174.7(1)	172.4(1)
	136.3(1)	129.8(1)

[a] Average distances. [b] Smallest and widest angles for Si1 or Si2, respectively. [c] M = Al. [d] M = Ga.

than the O···O distance in the intermolecular Si–OH···O*t*Bu interaction in the related silicate $[\mathrm{HC\{C(Me)N(2,6\text{-}}i\mathrm{Pr_2C_6H_3)\}_2]Al(SH)(\mu\text{-}O)Si(OH)(O}t\mathrm{Bu)_2}$[5a] (2.891(2) Å). However, they are significantly longer compared to those O···O distances in $[\mathrm{HC\{C(Me)N(2,6\text{-}}i\mathrm{Pr_2C_6H_3)\}_2]Ga(NHEt)(\mu\text{-}O)Si(OH)(O}t\mathrm{Bu)_2}$[5b] (2.753(2) Å) or in **a** (Si–OH···O(H)Al; 2.762(3) Å) and **b** (Si–OH···O(H)Ga; 2.705(4) Å) containing strong intramolecular hydrogen bonds. The hydrogen bonds found in **1** and **2** are the weakest in the series of related silicates (Table S1 in Supporting Information). The steric bulk around the metal atom in **1** and **2** results in one nearly linear M–O–Si angle (**1** 174.7(1)°, **2** (172.4(1)°), whereas the other is with 136.3(1)° (**1**) or 129.8(1)° (**2**) comparable to those found in **a** and **b** where the formation of the hydrogen bonds caused rather acute M–O–Si angles [132.8(1)° (**a**) and 128.9(2)° (**b**)]. The flexibility of the M–O–Si angle is well demonstrated by the values observed in the following related compounds: $[\mathrm{HC\{C(Me)N(2,6\text{-}}i\mathrm{Pr_2C_6H_3)\}_2]Al(SH)(\mu\text{-}O)Si(OH)(O}t\mathrm{Bu)_2}$ 146.5(1)°,[5a] $[(\mathrm{HC\{C(Me)N(2,6\text{-}}i\mathrm{Pr_2C_6H_3)\}_2)Al(SLi)(\mu\text{-}O)Si(OLi\cdot 2thf)(O}t\mathrm{Bu)_2]_2}$ 147.4(2)°,[5a] $[\mathrm{HC\{C(Me)N(2,6\text{-}}i\mathrm{Pr_2C_6H_3)\}_2]Ga(NHEt)(\mu\text{-}O)Si(OH)(O}t\mathrm{Bu)_2}$ 136.6(1)°, and $[\mathrm{HC\{C(Me)N(2,6\text{-}}i\mathrm{Pr_2C_6H_3)\}_2]Ga(Cl)(\mu\text{-}O)Si(OH)(O}t\mathrm{Bu)_2}$ 138.2(1)°.[5b] It is noteworthy that the second Si–OH group is not involved in any hydrogen bond due to its location between hydrocarbon groups (two *i*Pr and three *t*Bu groups) away from the inorganic core. This explains the stability of **1** and **2** in the solid state.

Consequently, the reactivities of **1** and **2** were explored with group 4 metal amides to determine the effect of one extra Si–O unit in the Si–O–M–O–Si–O–M′–O eight-membered ring on its flexibility and geometry when compared to the Si–O–

Table 2. Crystallographic Information for Compounds 1–11

	1	**2**	**3**	**4**	**5**	**6**
chemical formula	$C_{45}H_{79}AlN_2O_8Si_2$	$C_{45}H_{79}GaN_2O_8Si_2$	$C_{53}H_{97}AlN_4O_8Si_2Zr$	$C_{53}H_{97}GaN_4O_8Si_2Zr$	$C_{53}H_{97}AlHfN_4O_8Si_2$	$C_{53}H_{97}GaHfN_4O_8Si_2$
fw	859.26	902.00	1092.73	1135.47	1180.00	1222.74
space group	$P2_1/n$ (No. 14, variation)	$P2_1/n$ (No. 14, variation)	$P2_1/c$ (No. 14)	$P2_1/c$ (No. 14)	$P2_1/c$ (No. 14)	$P2_1/c$ (No. 14)
a/Å	14.278(2)	14.501(2)	12.4257(4)	12.4717(5)	12.4329(7)	12.4739(4)
b/Å	20.082(3)	19.850(2)	13.0671(5)	13.0571(5)	13.0387(7)	13.0290(4)
c/Å	17.910(2)	17.756(3)	37.4401(13)	37.4659(14)	37.4929(19)	37.5017(11)
β/deg	103.98(2)	102.88(2)	91.881(1)	91.955(1)	91.999(1)	92.158(1)
V/Å^3	4983.2(12)	4982.4(12)	6075.8(4)	6097.6(4)	6074.2(6)	6090.5(3)
Z	4	4	4	4	4	4
T/K	100(2)	100(2)	100(2)	100(2)	100(2)	100(2)
λ/Å	0.710 73	0.710 73	0.710 73	0.710 73	0.710 73	0.710 73
μ/mm^{-1}	0.138	0.649	0.285	0.702	1.821	2.235
ρ_{calcd}/g cm^{-3}	1.145	1.202	1.195	1.237	1.290	1.333
R1 ($I > 2\sigma(I)$)[a]	0.0529	0.0326	0.0297	0.0296	0.0291	0.0188
wR2 (all data)[b]	0.1285	0.0844	0.0721	0.0701	0.0626	0.0427
	7·2.73toluene	**8**·2.88toluene	**9**·1.12toluene·0.38hexane	**10**·2.83toluene	**11**·1.378hexane·0.122toluene	
chemical formula	$C_{109.11}H_{175.84}Al_2N_4O_{16}Si_4Ti$	$C_{110.16}H_{177.04}Al_2N_4O_{16}Si_4Zr$	$C_{99.38}H_{172.75}Ga_2N_4O_{16}Si_4Zr$	$C_{109.81}H_{176.64}Al_2HfN_4O_{16}Si_4$	$C_{99.12}H_{174.26}Ga_2HfN_4O_{16}Si_4$	
fw	2013.92	2071.06	2022.68	2153.72	2108.45	
space group	$P2_1/n$ (No. 14, variation)	$P2_1/n$ (No. 14, variation)	$P2_1/c$ (No. 14)	$P2_1/n$ (No. 14, variation)	$P2_1/c$ (No. 14)	
a/Å	12.7898(13)	12.768(2)	13.7916(3)	12.777(2)	13.8092(9)	
b/Å	46.817(5)	46.784(5)	33.8092(8)	46.851(5)	33.807(2)	
c/Å	19.4595(19)	19.654(3)	24.2899(6)	19.643(2)	24.3049(15)	
β/deg	90.127(2)	90.24(3)	101.304(1)	90.32(2)	101.2160(10)	
V/Å^3	11652(2)	11740(3)	11106.3(5)	11758(3)	11130.1(12)	
Z	4	4	4	4	4	
T/K	100(2)	100(2)	100(2)	100(2)	100(2)	
λ/Å	0.710 73	0.710 73	0.710 73	0.710 73	0.710 73	
μ/mm^{-1}	0.190	0.209	0.676	1.002	1.513	
ρ_{calcd}/g cm^{-3}	1.148	1.172	1.210	1.217	1.258	
R1 ($I > 2\sigma(I)$)[a]	0.0530	0.0615	0.0346	0.0415	0.0496	
wR2 (all data)[b]	0.1298	0.1464	0.0875	0.0935	0.0955	

[a] $R1 = \Sigma||F_o| - |F_c||/\Sigma|F_o|$. [b] $wR2 = [\Sigma w(F_o^2 - F_c^2)^2/\Sigma(F_o^2)^2]^{1/2}$.

Scheme 2. Synthesis of Compounds 3−11

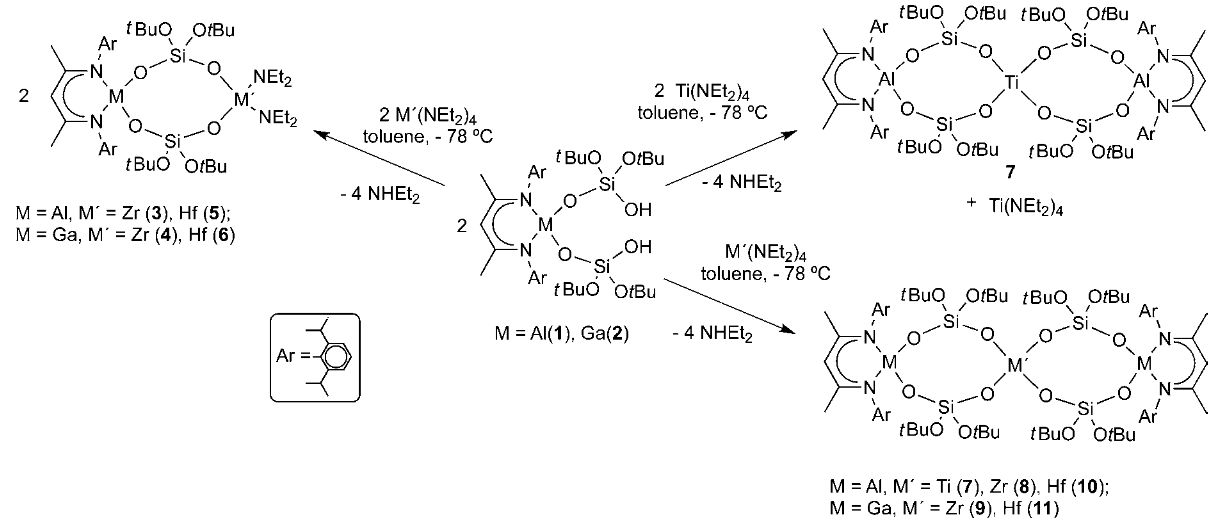

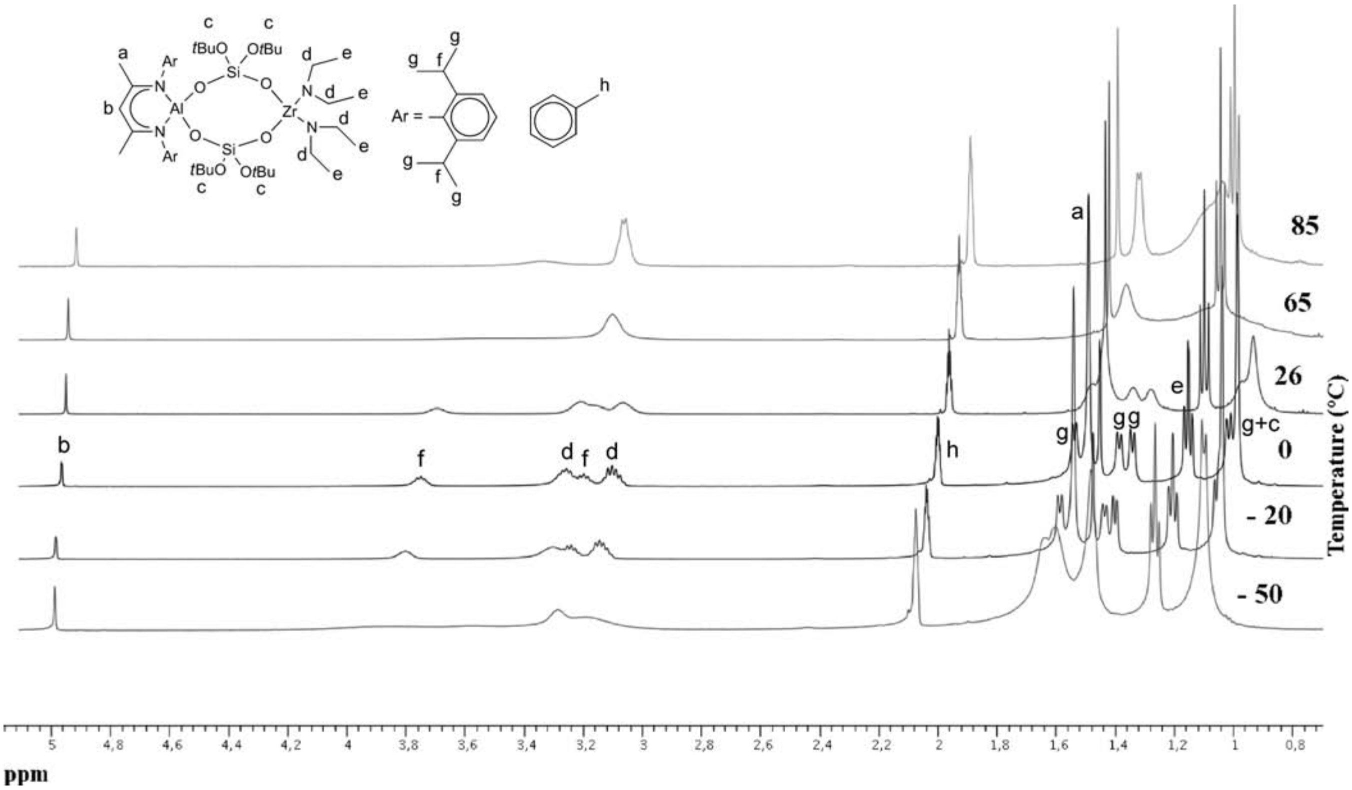

Figure 3. VT-500 MHz ^{1}H NMR spectra of compound **3** in toluene-d_8, in the 5.2−0.8 ppm region. Peaks are assigned for the spectrum measured at 0 °C.

M−O−M′−O six-membered rings based on **a** and **b**.[3b,c] The high oxophilicity of group 4 metals, the high reactivity of their amides, and the relevance of zeolites modified with group 4 metals in catalytic processes were relevant factors for the choice of these metals.[1b,g−i] Furthermore, their stable tetrahedral coordination environment can help to create 4R rings with the same coordination numbers observed in zeolites. Thus, reactions between 1 or 0.5 equiv of a group 4 amide M′$(NEt_2)_4$ (M′ = Ti, Zr, Hf) and **1** or **2** were performed. The equimolar reactions led to the isolation of four crystalline solids for the heavier group 4 metals with formulas $[HC\{C(Me)N(2,6\text{-}i\text{Pr}_2C_6H_3)\}_2]M[(\mu\text{-O})Si(\mu\text{-O})(OtBu)_2]_2M'(NEt_2)_2$ [M′ = Zr, M = Al (**3**), Ga (**4**); M′ = Hf, M = Al (**5**), Ga (**6**)] and the desired 4R topology. However, the reaction between $Ti(NEt_2)_4$ and compound **1** always resulted in the formation of the spiro-cyclic compound $\{[HC\{C(Me)N(2,6\text{-}i\text{Pr}_2C_6H_3)\}_2]Al[(\mu\text{-O})Si(\mu\text{-O})(OtBu)_2]_2\}_2Ti$ (**7**). The titanium derivatives $[HC\{C(Me)N(2,6\text{-}i\text{Pr}_2C_6H_3)\}_2]M[(\mu\text{-O})Si(\mu\text{-O})(OtBu)_2]_2Ti(NEt_2)_2$ (M = Al, Ga) could not be isolated even with a large excess of the amide. Such reactions resulted mainly in the decomposition of **1** and **2** as confirmed by ^{1}H NMR analysis. However, the use of 0.5 equiv of amide toward **1** or **2** led to the clean isolation of **7** and four other spiro-cyclic derivatives $\{[HC\{C(Me)N(2,6\text{-}i\text{Pr}_2C_6H_3)\}_2]M[(\mu\text{-}$

Table 3. Selected Bond Lengths [Å] and Angles [deg] for the Inorganic Rings in Compounds 3−6

distance (Å)	$3^{b,d}$	$4^{c,d}$	$5^{b,e}$	$6^{c,e}$	angle (deg)	$3^{b,d}$	$4^{c,d}$	$5^{b,e}$	$6^{c,e}$
M′−O(Si)	1.970(1)	1.967(1)	1.949(2)	1.952(1)	O−Si−O	110.8(1)	112.4(1)	110.6(1)	111.4(1)
	1.970(1)	1.970(1)	1.954(2)	1.952(1)		112.5(1)	113.5(1)	112.4(1)	113.4(1)
M−O(Si)	1.702(1)	1.781(1)	1.704(2)	1.782(1)	M′−O−Si	152.3(1)	152.0(1)	152.2(1)	151.7(1)
	1.721(1)	1.803(1)	1.721(2)	1.803(1)		155.1(1)	157.3(1)	155.5(1)	157.8(1)
Si−O(M′)	1.624(1)	1.624(1)	1.629(2)	1.625(1)	M−O−Si	151.1(1)	145.6(1)	150.8(1)	145.4(1)
	1.623(1)	1.625(1)	1.624(2)	1.627(1)		159.7(1)	157.6(1)	159.8(1)	157.9(1)
Si−O(M)	1.601(1)	1.599(1)	1.600(2)	1.599(1)	O−M−O	108.9(1)	108.7(1)	108.9(1)	109.0(1)
	1.605(1)	1.600(1)	1.606(2)	1.598(1)	N−M−N	103.6(1)	103.4(1)	103.9(1)	103.9(1)
M′−N[a]	2.038(2)	2.038(2)	2.024(2)	2.027(2)	O−E−O	116.1(1)	116.8(1)	115.9(1)	116.6(1)
M−N[a]	1.902(2)	1.938(2)	1.902(3)	1.936(2)					
Si−O(O*t*Bu)[a]	1.634(1)	1.634(2)	1.635(2)	1.634(2)					

[a] Average bond lengths. [b] M = Al. [c] M = Ga. [d] M′ = Zr. [e] M′ = Hf.

Table 4. Selected Bond Lengths [Å] and Angles [deg] for the Inorganic Rings in Compounds 7−11

distance (Å)	$7^{b,d}$	$8^{b,e}$	$9^{c,e}$	$10^{b,f}$	$11^{c,f}$	angle (deg)	$7^{b,d}$	$8^{b,e}$	$9^{c,e}$	$10^{b,f}$	$11^{c,f}$
M′−O(Si)	1.792(1)	1.928(2)	1.938(2)	1.920(2)	1.931(3)	O−M′−O	106.4(1)	104.6(1)	104.7(1)	105.3(1)	105.2(1)
	1.799(1)	1.943(2)	1.948(2)	1.933(2)	1.939(3)		106.8(1)	105.2(1)	105.9(1)	106.0(1)	106.4(1)
	1.802(1)	1.943(2)	1.945(2)	1.934(2)	1.940(3)	O−M−O	112.4(1)	113.4(1)	112.7(1)	113.3(1)	112.6(1)
	1.808(1)	1.950(2)	1.952(2)	1.942(2)	1.944(3)		112.4(1)	113.4(1)	114.8(1)	113.5(1)	114.6(1)
M−O(Si)	1.700(1)	1.698(2)	1.796(2)	1.701(2)	1.789(3)	O−Si−O	109.9(1)	109.7(1)	112.3(1)	109.9(1)	110.1(1)
	1.708(1)	1.706(2)	1.784(2)	1.712(2)	1.791(3)		110.8(1)	111.0(1)	111.2(1)	111.0(1)	111.4(1)
	1.718(1)	1.713(2)	1.805(2)	1.719(2)	1.798(3)		110.9(1)	111.0(1)	112.2(1)	111.1(1)	112.3(1)
	1.720(1)	1.718(2)	1.786(2)	1.720(2)	1.805(3)		111.2(1)	111.0(1)	110.1(1)	111.1(1)	112.4(1)
Si−O(M′)	1.635(1)	1.625(2)	1.628(2)	1.626(2)	1.626(3)	M′−O−Si	155.4(1)	152.8(1)	156.7(1)	152.8(1)	156.4(1)
	1.636(1)	1.627(2)	1.638(2)	1.629(2)	1.628(3)		157.0(1)	155.0(1)	159.1(1)	154.8(1)	156.5(1)
	1.646(1)	1.631(2)	1.629(2)	1.633(2)	1.631(3)		158.1(1)	158.0(1)	158.2(1)	157.2(1)	157.7(2)
	1.647(1)	1.636(2)	1.633(2)	1.636(2)	1.636(3)		158.7(1)	159.0(1)	156.4(1)	158.6(1)	158.6(2)
Si−O(M)	1.594(1)	1.592(2)	1.595(2)	1.593(2)	1.594(3)	M−O−Si	151.9(1)	151.0(1)	154.4(1)	150.9(1)	152.5(2)
	1.594(1)	1.599(2)	1.597(2)	1.594(2)	1.594(3)		155.5(1)	155.8(1)	152.5(1)	155.9(1)	153.4(2)
	1.599(1)	1.600(2)	1.595(2)	1.602(2)	1.595(3)		156.7(1)	158.6(1)	153.0(1)	158.5(1)	154.3(2)
	1.599(1)	1.603(2)	1.595(2)	1.605(2)	1.595(3)		158.9(1)	161.7(1)	156.2(1)	161.3(1)	156.1(2)
M−N[a]	1.911(2)	1.907(3)	1.948(2)	1.908(3)	1.948(4)						
Si−O(*t*Bu)[a]	1.626(1)	1.625(2)	1.630(2)	1.627(2)	1.628(3)						

[a] Average bond lengths. [b] M = Al. [c] M = Ga. [d] M′ = Ti. [e] M′ = Zr. [f] M′ = Hf.

O)Si(μ-O)(O*t*Bu)$_2$]$_2$}$_2$M′ [M′ = Zr, M = Al (**8**), Ga (**9**); M′ = Hf, M = Al (**10**), Ga (**11**)] with spiro-4R topology (Scheme 2). Until now, we have not been able to isolate any titanium derivative of **2**. This is probably due to the high acidity of titanium and weaker Ga−O bonds when compared to the Al−O bond energy. Compounds **3**−**11** are highly soluble in organic solvents including hexane, which makes their isolation rather difficult and leads to lower yields.

The absence of signals for the −OH groups in IR and ^{1}H NMR spectra of **3**−**6** together with the presence of signals for the NEt$_2$ substituents confirmed the deprotonation of the silanol moieties and the concomitant formation of the M′−O bonds. The ^{1}H NMR spectra of the heterometallic derivatives exhibit broad signals at room temperature. This was attributed to a fluxional behavior caused by the flexible eight-membered rings. In consequence, low temperature ^{1}H NMR experiments were performed for all compounds observing decoalescence for most of the signals in the spectra in the range 0 to −10 °C with a pattern that corresponds to C_{2v} or D_{4h} symmetries for the cyclic (**3**−**6**) and spiro-cyclic (**7**−**11**) derivatives, respectively. Full variable temperature ^{1}H NMR experiments were performed for **3** and **7** between −50 (for **3**) or −70 (for **7**) and 85 °C, respectively (Figure 3). However, even in this range, full coalescence or decoalescence of the signals could not be observed. This confirms the high flexibility of the inorganic rings at low temperature, but also the steric bulk of the ligand **L**, which prevents the coalescence at high temperatures (Figures S1−S12 in Supporting Information).

The cyclic derivatives **3**−**6** crystallized from toluene in the monoclinic space group $P2_1/c$ with one molecule of the corresponding compound in the asymmetric unit and are isomorphous. The alumodisilicate spirocyclic derivatives **7**, **8**, and **10** are isomorphous and crystallized from toluene in the monoclinic space group $P2_1/n$ with one molecule of the particular compound and 2.73, 2.88, or 2.83 molecules of toluene, respectively, in the asymmetric unit. Finally, **9** and **11** crystallized from a hexane/toluene mixture in the monoclinic space group $P2_1/c$, with one molecule of the compound and a mixture of hexane and toluene (together 1.5 molecules) in the asymmetric unit (Tables 2−4, Figure 4).

All compounds exhibit eight-membered inorganic rings with M(O−Si−O)$_2$M′ connectivity in a boat−chair conformation for the cyclic derivatives **3**−**6** and two almost perpendicular diplanar rings for the spirocyclic compounds **7**−**11**. It is noteworthy that the size of the spirocyclic inorganic cores is 0.81 nm. The bond lengths in the inorganic rings are similar for both cyclic and spirocyclic compounds, and the size is related to the acidity of the metal atom M′(IV) or M(III) present in the

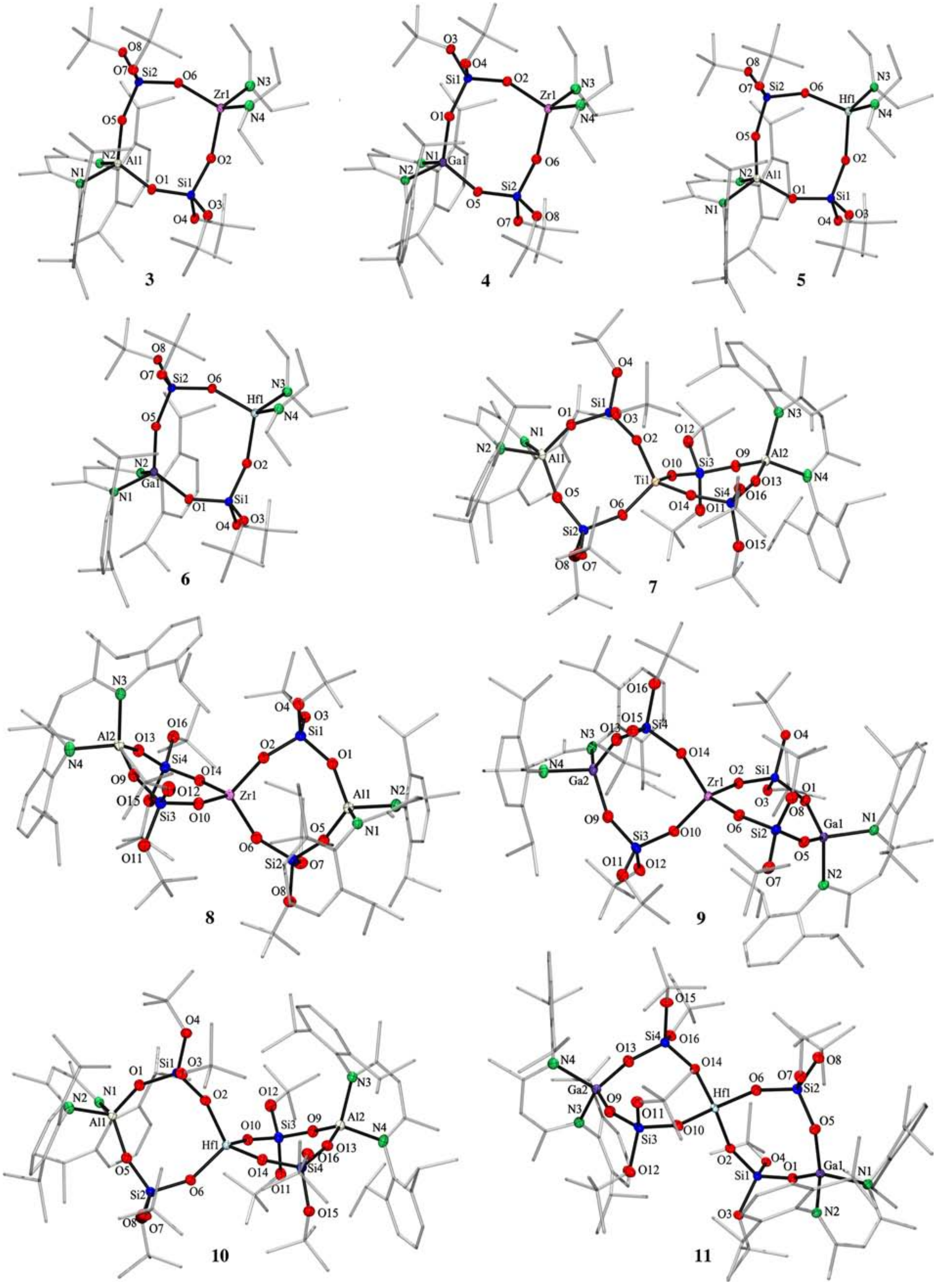

Figure 4. Molecular structures of **3**−**11**. Carbon ellipsoids and carbon-bound hydrogen atoms have been omitted for clarity. Thermal ellipsoids of noncarbon atoms are set at 50% probability level.

molecule, where shorter distances for the more acidic atoms are observed. Thus, M′−O bond lengths for the heavier M′(IV) zirconium and hafnium compounds are similar (1.931(3) Å ≤ M′−O ≤ 1.970(1) Å, for **3**−**6**, **8**−**11**) but longer than those found in the titanium spiro-cycle 7 (1.792(1) Å ≤ Ti−O ≤ 1.808(1) Å). Nevertheless, those distances are similar to the related tetracoordinated group 4 alumo- and gallosilicates $[HC\{C(Me)N(2,6\text{-}iPr_2C_6H_3)\}_2]M(\mu\text{-}O)_2Si(\mu\text{-}O)(OtBu)_2M'(NR_2)_2$ or $[(HC\{C(Me)N(2,6\text{-}iPr_2C_6H_3)\}_2)M(\mu\text{-}O)_2Si(\mu\text{-}O)(OtBu)_2]_2M'$ (M′ = Zr or Hf, M = Al, 1.961(2) Å ≤ M′−O ≤ 1.987(1) Å; M = Ga, 1.952(3) Å ≤ M′−O ≤ 1.989(2) Å and M′ = Ti, M = Al, 1.832(2) Å ≤ Ti−O ≤ 1.842(2) Å),[5b,c] as well as to the tetra- and pentacoordinated group 4 silicates $M'[OSi(OtBu)_3]_4$, $M'[OSi(\mu\text{-}OtBu)(OtBu)_2][OSi(OtBu)_3]_3$ (1.945(6) ≤ Zr−O ≤ 2.038(6);[20a] 1.912(4) ≤ Hf−O ≤ 2.021(4)[20a,b] Å) and $[(tBuO)_2Ti\{\mu\text{-}O_2Si[OSi(OtBu)_3]_2\}]_2$ (1.812(4) ≤ Ti−O ≤ 1.816(4) Å).[7n] The M−O bond distances for the heterobimetallic alumodisilicates **3**, **5**, **7**, **8**, **10** (1.700(1) Å ≤ Al−O ≤ 1.721 (2) Å) are shorter than those found in the gallodisilicates **4**, **6**, **9**, **11** (1.781(1) Å ≤ Ga−O ≤ 1.805(3) Å) and in both cases comparable to those in the related group 4 alumo- and gallosilicate derivatives $[HC\{C(Me)N(2,6\text{-}iPr_2C_6H_3)\}_2]M(\mu\text{-}O)_2Si(\mu\text{-}O)(OtBu)_2M'(NR_2)_2$ or $[(HC\{C(Me)N(2,6\text{-}iPr_2C_6H_3)\}_2)M(\mu\text{-}O)_2Si(\mu\text{-}O)(OtBu)_2]_2M'$ (M′ = Ti, Zr or Hf, M = Al, 1.716(2) Å ≤ Al−O ≤ 1.732(1) Å; M = Ga, 1.800(2) Å ≤ Ga−O ≤ 1.817(3) Å).[5b,c] They are also similar to those found in the alumosilicates $Al[OSi(OtBu)_3]_3(iPrOH)\cdot 1/2[Al(OiPr)_3]_4$, $[(OiPr)_2AlOSi(OtBu)_3]_2$, $\{[HC\{C(Me)N(2,6\text{-}iPr_2C_6H_3)\}_2]Al(\mu\text{-}O)[(tBuO)_2Si](\mu\text{-}O)\}_2$, and the silicoalumophosphate $[(tBuO)_3SiO]_2Al[(\mu\text{-}O)_2P(OtBu)_2]_2Al(Me)\text{-}OSi(OtBu)_3$ (1.684(6) ≤ Al−O ≤ 1.721(2) Å),[7n,21a,b] and are in the range observed in the mineral gismondine (Al−O ∼ 1.74 Å)[20a] or the synthetic zeolites ABW ($LiMSiO_4\cdot H_2O$, M = Al, Ga; Al−O ∼ 1.75 Å, Ga−O ∼ 1.804(4) Å, respectively)[22b] but shorter than those in the bridged system$\{Me_2Al[\mu\text{-}OSi(OtBu)_3]_2\}$[21c] (Al−O ∼ 1.865(4) Å). In all compounds, the geometry of the silicate moiety remains almost unchanged as is evidenced by similar Si−O bond lengths in all compounds (1.623(1) Å ≤ Si−O(M′) ≤ 1.647.(1) Å, 1.593(2) Å ≤ Si−O(M) ≤ 1.606(2) Å, for **3** − **11**), which are comparable to the average distance in several zeolite frameworks (1.61 Å).[22] The angles in the inorganic rings are similar for all the compounds although a higher flexibility is observed in the gallodisilicate derivatives (**4**, **6**, **9**, **11**) due the longer Ga−O bonds: M′−O−Si (151.7(1)−159.1(1)°) and the Ga−O−Si (145.4(1)−157.9(1)°) angles compared to the respective alumodisilicates (**3**, **5**, **8**, **10**) M′−O−Si (152.2(1)−155.5(1)°) and Al−O−Si (150.8(1)−159.8(1)°) angles. Nevertheless, similar O−M−O (112.4(1)−116.8(1)°), O−M′−O (104.6(1)−109.0(1)°) and O−Si−O (109.7(1)−113.5(1)°) angles are found in both systems. The angles observed in **3**−**11** are similar to those found in the eight membered cycles present in the titanosilicate $[(tBuO)_2Ti\{\mu\text{-}O_2Si[OSi(OtBu)_3]_2\}]_2$,[13] the alumosilicate $\{[HC\{C(Me)N(2,4,6\text{-}Me_3C_6H_2)\}_2]Al(\mu\text{-}O)[(tBuO)_2Si](\mu\text{-}O)\}_2$,[7n] and the alumoazasilicates $[(2,6\text{-}iPr_2C_6H_3)N(SiMe_3)Si(OH)O_2Al(iBu)\cdot thf]_2$, $[(2,6\text{-}iPr_2\text{-}C_6H_3)N(SiMe_2iPr)SiO_3Al\cdot thf]_4$, $[(2,6\text{-}Me_2\text{-}C_6H_3)N(SiMe_3)SiO_3Al\cdot thf]_4$, and $[(2,6\text{-}Me_2\text{-}C_6H_3)N(SiMe_3)SiO_3Al\cdot 1,4\text{-}dioxane]_4$[23] (109.4(2)° ≤ O−Ti−O ≤ 110.0(2)°, 113.2(1)° ≤ O−Al−O ≤ 117.6(1)°, and 108.9(2)° ≤ O−Si−O ≤ 113.7(1)°). Finally, the linear or terminal group 4 silicates $M'[OSi(OtBu)_3]_4$ (M′ = Zr, Hf)[5a,b] and alumosilicates $Al[OSi(OtBu)_3]_3(iPrOH)\cdot 1/2[Al(OiPr)_3]_4$,[21a] $[(OiPr)_2AlOSi(OtBu)_3]_2$,[21b] and $\{Me_2Al[\mu\text{-}OSi(OtBu)_3]_2\}$[21c] present more obtuse angles (108.2(4)° ≤ O−M′−O ≤ 110.0(2)°, 113.9(1)° ≤ O−Al−O ≤ 119.1(3)°, and 104.7(1)° ≤ O−Si−O ≤ 117.9(7)°) than those in **3**−**11**.

■ CONCLUSION

The stabilization of the first metallodisilicates based on aluminum and gallium with two terminal Si−OH groups was achieved by kinetic control using a bulky β-diketiminate ligand and protecting O*t*Bu groups. The compounds have been successfully used in the preparation of cyclic and spirocyclic heterobimetallic silicates containing group 4 metals and 4R rings known from zeolites. The spirocyclic compounds feature unique inorganic silicate cores of 0.81 nm, and neither of these compounds have any precedent in the literature. The disilicates **1** and **2** are proposed to be models for vicinal −OH groups on silica surface.

■ ASSOCIATED CONTENT

Ⓢ Supporting Information

Additional crystallographic details (including data in CIF format) and ^1H NMR and IR spectra. This material is available free of charge via the Internet at http://pubs.acs.org.

■ AUTHOR INFORMATION

Corresponding Author

*E-mail: vjancik@unam.mx. Fax: (+) 52-55-5616-2217.

Author Contributions

The manuscript was written through contributions of all authors. All authors have given approval to the final version of the manuscript.

Notes

The authors declare no competing financial interest.

■ ACKNOWLEDGMENTS

The financial support from DGAPA-UNAM (PAPIIT Grant IN211910) and CONACyT (Grant 79531) is gratefully acknowledged. R.H.-L. and D.S.-I. gratefully acknowledge the Ph.D. fellowships provided by CONACyT (Grants 195791 and 268796, respectively). Alejandra Núñez-Pineda and Lizbeth Triana Cruz are gratefully acknowledged for their technical support.

■ REFERENCES

(1) (a) Breck, D. *Zeolite Molecular Sieves: Structure, Chemistry, and Use*; Wiley: New York, 1974. (b) Bhatia, S. *Zeolite Catalysis: Principles and Applications*; CRC Press: Boca Raton, FL, 1990. (c) Čejka, J.; Mintova, S. *Catal. Rev.* **2007**, *49*, 457−509. (d) Ackley, M. W.; Rege, S. U.; Saxena, H. *Microporous Mesoporous Mater.* **2003**, *61*, 25−42. (e) Davis, M. E. *Nature* **2002**, *417*, 813−821. (f) Baerlocher, C.; McCusker, L. B.; Olson, D. *Atlas of Zeolite Framework Types*; Elsevier Science: New York, 2007. (g) Grey, R. A.; Pitchai, R. U.S. Patent US6194591, 2001. (h) Wang, Y.; Zhang, A.; Xu, Q.; Chen, R. *Appl. Catal., A* **2001**, *214*, 167−177. (i) Sheldon, R. A. *Stud. Surf. Sci. Catal.* **1990**, *55*, 1.

(2) (a) Gerritsen, G.; Duchateau, R.; Yap, G. *Organometallics* **2003**, *22*, 100−110. (b) Duchateau, R.; Dijkstra, T.; van Santen, R.; Yap, G. *Chem.—Eur. J.* **2004**, *10*, 3979−3990. (c) Boscoboinik, J. A.; Yu, X.; Yang, B.; Fischer, F. D.; Wlodarczyk, R.; Sierka, M.; Shaikhutdinov, S.; Sauer, J.; Freund, H.-J. *Angew. Chem., Int. Ed.* **2012**, *51*, 6005−6008.

(3) (a) Hoffmann, F.; Cornelius, M.; Morell, J.; Fröba, M. *Angew. Chem., Int. Ed.* **2006**, *45*, 3216−3251. (b) Hunt, J. R.; Doonan, C. J.; LeVangie, J. D.; Côté, A. P.; Yaghi, O. M. *J. Am. Chem. Soc.* **2008**, *130*, 11872−11873. (c) Davies, R. P.; Lickiss, P. D.; Robertson, K.; White, A. J. P. *CrystEngComm* **2012**, *14*, 758−760. (d) Davies, R. P.; Less, R. J.; Lickiss, P. D.; Robertson, K.; White, A. J. P. *Inorg. Chem.* **2008**, *47*, 9958−9964. (e) Bellussi, G.; Montanari, E.; Di Paola, E.; Millini, R.; Carati, A.; Rizzo, C.; O'Neil Parker, W., Jr.; Gemmi, M.; Mugnaioli, E.; Kolb, U.; Zanardi, S. *Angew. Chem., Int. Ed.* **2011**, *51*, 690−693.

(f) Bellussi, G.; Carati, A.; Di Paola, E.; Millini, R.; Parker, W. O. N.; Rizzo, C.; Zanardi, S. *Microporous Mesoporous Mater.* **2008**, *113*, 252−260.

(4) Kerr, J. A. In *CRC Handbook of Chemistry and Physics 1999−2000*; Lide, D. R., Ed.; CRC Press: Boca Raton, FL, 2000.

(5) (a) Jancik, V.; Rascón-Cruz, F.; Cea-Olivares, R.; Toscano, R. A. *Chem. Commun.* **2007**, 4528−4530. (b) Solis-Ibarra, D.; Velásquez-Hernández, M. de J.; Huerta-Lavorie, R.; Jancik, V. *Inorg. Chem.* **2011**, *50*, 8907−8917. (c) Huerta-Lavorie, R.; Rascón-Cruz, F.; Solis-Ibarra, D.; Zavala-Segovia, N.; Jancik, V. *Eur. J. Inorg. Chem.* **2011**, 4795−4799.

(6) (a) Beckmann, J.; Mahieu, B.; Nigge, W.; Schollmeyer, D.; Schurmann, M.; Jurkschat, K. *Organometallics* **1998**, *17*, 5697−5712. (b) Hossain, M. A.; Hursthouse, M. B.; Mazid, M. A.; Sullivan, A. C. *Chem. Commun.* **1988**, 1305−1306. (c) Veith, M.; Vogelgesang, H.; Huch, V. *Organometallics* **2002**, *21*, 380−388. (d) Hossain, M. A.; Hursthouse, M. B.; Ibrahim, A.; Mazid, M. A.; Sullivan, A. C. *J. Chem. Soc., Dalton Trans.* **1989**, 2347−2352. (e) Hoebbel, D.; Nacken, M.; Schmidt, H.; Huch, V.; Veith, M. *J. Mater. Chem.* **1998**, *8*, 171−178. (f) Lorenz, V.; Fischer, A.; Jacob, K.; Bruser, W.; Gelbrich, T.; Jones, P. G.; Edelmann, F. T. *Chem. Commun.* **1998**, 2217−2218. (g) Lorenz, V.; Fischer, A.; Jacob, K.; Bruser, W.; Edelmann, F. T. *Chem.—Eur. J.* **2001**, *7*, 848−857. (h) Gun'ko, Y. K.; Reilly, R.; Kessler, V. G. *New J. Chem.* **2001**, *25*, 528−530. (i) Kapoor, R. N.; Cervantes-Lee, F.; Campana, C. F.; Haltiwanger, C.; Abney, K.; Pannell, K. H. *Inorg. Chem.* **2006**, *45*, 2203−2208. (j) Lazell, M.; Motevalli, M.; Shah, S. A. A.; Simon, C. K. S.; Sullivan, A. C. *J. Chem. Soc., Dalton Trans.* **1996**, 1449−1454.

(7) (a) Nolte, J.-O.; Schneider, M.; Neumann, B.; Stammler, H.-G.; Jutzi, P. *Organometallics* **2003**, *22*, 1010−1017. (b) Beckmann, J.; Jurkschat, K.; Schurmann, M.; Dakternieks, D.; Lim, A. E. K.; Lim, K. F. *Organometallics* **2001**, *20*, 5125−5133. (c) Puff, H.; Bockmann, M. P.; Kok, T. R.; Schuh, W. *J. Organomet. Chem.* **1984**, *268*, 197−206. (d) Samuel, E.; Harrod, J. F.; McGlinchey, M. J.; Cabestaing, C.; Robert, F. *Inorg. Chem.* **1994**, *33*, 1292−1296. (e) Ohde, C.; Brandt, M.; Limberg, C.; Dobler, J.; Ziemer, B.; Sauer, J. *Dalton Trans.* **2008**, 326−331. (f) Mazzah, A.; Haoudi-Massah, A.; Noltemeyer, M.; Roesky, H. W. *Z. Anorg. Allg. Chem.* **1991**, *604*, 93−103. (g) Beckmann, J.; Jurkschat, K.; Kaltenbrunner, U.; Pieper, N.; Schurmann, M. *Organometallics* **1999**, *18*, 1586−1595. (h) Liu, F.-Q.; Uson, I.; Roesky, H. W. *Z. Anorg. Allg. Chem.* **1996**, *622*, 819−822. (i) Vennat, M.; Herson, P.; Bregeault, J.-M.; Shul'pin, G. B. *Eur. J. Inorg. Chem.* **2003**, 908−917. (j) Haoudi-Mazzah, A.; Mazzah, A.; Schmidt, H.-G.; Noltemeyer, M.; Roesky, H. W. *Z. Naturforsch., B: Chem. Sci.* **1991**, *46*, 587−592. (k) Haoudi-Mazzah, A.; Dhamelincourt, P.; Mazzah, A.; Lazraq, M. *J. Raman Spectrosc.* **1998**, *29*, 1047−1053. (l) Brutchey, R. L.; Mork, B. V.; Sirbuly, D. J.; Yang, P.; Tilley, T. D. *J. Mol. Catal. A: Chem.* **2005**, *238*, 1−12. (m) Reyes-Garcia, E. A.; Cervantes-Lee, F.; Pannell, K. H. *Organometallics* **2001**, *20*, 4734−4740. (n) González-Gallardo, S.; Jancik, V.; Delgado-Robles, A. A.; Moya-Cabrera, M. *Inorg. Chem.* **2011**, *50*, 4226−4228.

(8) Gosink, H.-G.; Roesky, H. W.; Schmidt, H.-G.; Noltemeyer, M.; Irmer, E.; Herbst-Irmer, R. *Organometallics* **1994**, *13*, 3420−3426.

(9) Klemp, A.; Hatop, H.; Roesky, H. W.; Schmidt, H.-G.; Noltemeyer, M. *Inorg. Chem.* **1999**, *38*, 5832−5836.

(10) Balkenhol, D.; Beckmann, J.; Jurkschat, K.; Schürmann, M. *Z. Anorg. Allg. Chem.* **2004**, *630*, 1875−1878.

(11) (a) Feher, F. J. *J. Am. Chem. Soc.* **1986**, *108*, 3850−3852. (b) Gun'ko, Y. K.; Kessler, V. G.; Reilly, R. *Inorg. Chem. Commun.* **2004**, *7*, 341−343. (c) Feher, F. J.; Newman, D. A.; Walzer, J. F. *J. Am. Chem. Soc.* **1989**, *111*, 1741−1748. (d) Spirk, S.; Nieger, M.; Belaj, F.; Pietschnig, R. *Dalton Trans.* **2009**, 163−167. (e) Feher, F. J.; Terroba, R.; Ziller, J. W. *Chem. Commun.* **1999**, 2153−2154. (f) Feher, F. J.; Terroba, R.; Ziller, J. W. *Chem. Commun.* **1999**, 2309−2310. (g) Liu, H.; Kondo, S.; Tanaka, R.; Oku, H.; Unno, M. *J. Organomet. Chem.* **2008**, *693*, 1301−1308. (h) Jones, M. D.; Keir, C. G.; Johnson, A. L.; Mahon, M. F. *Polyhedron* **2010**, *29*, 312−316.

(12) (a) Graalmann, O.; Klingebiel, U.; Clegg, W.; Haase, M.; Sheldrick, G. M. *Chem. Ber.* **1984**, *117*, 2988−2997. (b) Beckmann, J.; Dakternieks, D.; Duthie, A.; Foitzik, R. C. *Silicon Chem.* **2003**, *2*, 27−36. (c) Behbehani, H.; Brisdon, B. J.; Mahon, M. F.; Molloy, K. C.; Mazhar, M. *J. Organomet. Chem.* **1993**, *463*, 41−45. (d) Malinovsky, S. T.; Vallina, A. T.; Stoeckli-Evans, H. *Zh. Strukt. Khim.* **2006**, *47*, 1143−1149.

(13) Beckmann, J.; Dakternieks, D.; Duthie, A.; Larchin, M. L.; Tiekink, E. R. T. *Appl. Organomet. Chem.* **2003**, *17*, 52−62.

(14) (a) Cui, C.; Roesky, H. W.; Hao, H.; Schmidt, H.-G.; Noltemeyer, M. *Angew. Chem.* **2000**, *112*, 1885−1887; *Angew. Chem., Int. Ed.* **2000**, *39*, 1815−1817. (b) Solis-Ibarra, D.; Gómora-Figueroa, A. P.; Zavala-Segovia, N.; Jancik, V. *Eur. J. Inorg. Chem.* **2009**, 4564−4571. (c) Bradley, D.; Thomas, I. *J. Chem. Soc.* **1960**, *137*, 3857−3861.

(15) The molecular weight of compounds **3**−**11** exceeds the *m*/*z* range of the Shimadzu GCMS-QP2010 Plus spectrometer (35−1090 *m*/*z*) used for the EI-MS characterization of **1** and **2**.

(16) *SAINT and SADABS*; Bruker AXS Inc.: Madison, WI, 2007.

(17) SHELX: Sheldrick, G. M. *Acta Crystallogr., Sect. A* **2008**, *64*, 112−122.

(18) SHELXLE: Hübschle, C. B.; Sheldrick, G. M.; Dittrich, B. *J. Appl. Crystallogr.* **2011**, *44*, 1281−1284.

(19) (a) Zhu, H.; Chai, J.; Jancik, V.; Roesky, H. W.; Merrill, W. A.; Power, P. P. *J. Am. Chem. Soc.* **2005**, *127*, 10170−10171. (b) Bai, G.; Roesky, H. W.; Li, J.; Noltemeyer, M.; Schmidt, H.-G. *Angew. Chem.* **2003**, *115*, 5660−5664; *Angew. Chem., Int. Ed.* **2003**, *42*, 5502−5506. (c) Muragavel, R.; Walawalkar, M. G.; Dan, M.; Roesky, H. W.; Rao, C. N. R. *Acc. Chem. Res.* **2004**, *37*, 763−774.

(20) (a) Terry, K. W.; Lugmair, C. G.; Tilley, T. D. *J. Am. Chem. Soc.* **1997**, *119*, 9745−9756. (b) Lugmair, C. G.; Tilley, T. D. *Inorg. Chem.* **1998**, *37*, 764−769.

(21) (a) Lugmair, C. G.; Fujdala, K. L.; Tilley, T. D. *Chem. Mater.* **2002**, *14*, 888−898. (b) Fujdala, K. L.; Tilley, T. D. *J. Am. Chem. Soc.* **2001**, *123*, 10133−10134. (c) Terry, K. W.; Ganzel, P. K.; Tilley, T. D. *Chem. Mater.* **1992**, *4*, 1290−1295.

(22) (a) Fischer, K. *Am. Mineral.* **1963**, *48*, 664−672. (b) Kerr, I. S. *Z. Kristallogr.* **1979**, *139*, 186−195. (c) Newsam, J. M. *J. Phys. Chem.* **1988**, *92*, 445−452.

(23) (a) Montero, M. L.; Usón, I.; Roesky, H. W. *Angew. Chem.* **1994**, *106*, 2198−2200. (c) *Angew. Chem., Int. Ed.* **1994**, *33*, 2103−2104. (b) Chandrasekhar, V.; Muragavel, R.; Voight, A.; Roesky, H. W.; Schmidt, H.-G.; Noltemeyer, M. *Organometallics* **1996**, *15*, 918−922.